Analysis of IGRF-13 geomagnetic field model candidates

Ingo Wardinski*[1]

[1]EOST Strasbourg, France

November 25, 2019

1 Naming and measures

This evaluation follows closely [4] and uses their equations 2, 3 and 6. [4] defines a rms vector difference field between two models (see their equation 7). In this evaluation the squared quantity is used and referenced as the total field intensity. **Because of their similarity, I guess this is also applied by F. Lowes in his preliminary analysis (email October 31., 2019).** Furthermore, we do not provide comparisons between individual candidates, like in table 3 of [4]. Simply because this would have lead to the discussion of 388 comparisons.

The difference between the arithmetic mean model of all candidates and an individual candidate are referred to as the difference field. Finally, Model names are those of P. Alken.

2 DGRF 2015 candidate models

Figure 1 shows the radial component of the equally weighted average field of all DGRF candidates.

A first inspection of differences between mean and candidate models shows that the differences of individual Gauss coefficients rarely exceed 1 nT, see Figure 2. Most largest deviations occur for the first spherical harmonic degrees. From spherical harmonic degree 6 onward, none of the candidates show differences to the mean field larger than 0.5 nT.

Table 1 summarizes the total field intensity of the differences between a candidate model and the mean field model. The computation of these quanties follows [4]. However, these values differ from those of Alken and Lowes, as only two decimal places are considered.

*wardinski@unistra.fr

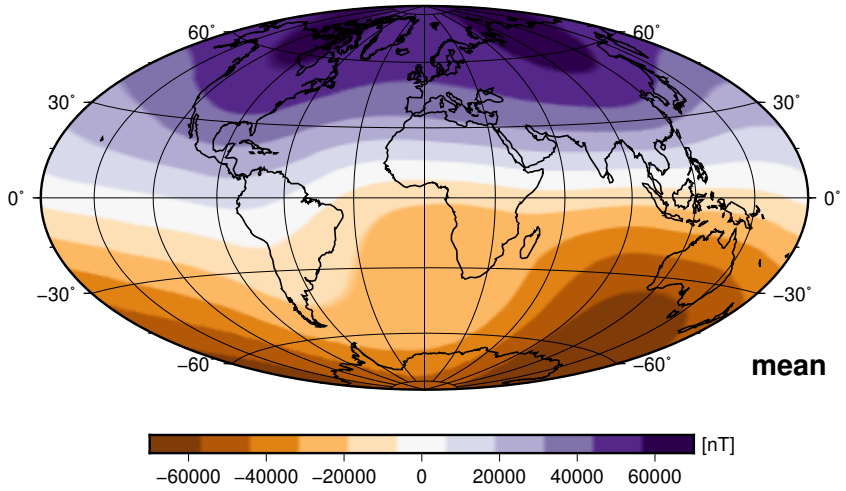

Figure 1: Radial component of the mean field at Earth's surface derived from all DGRF candidates.

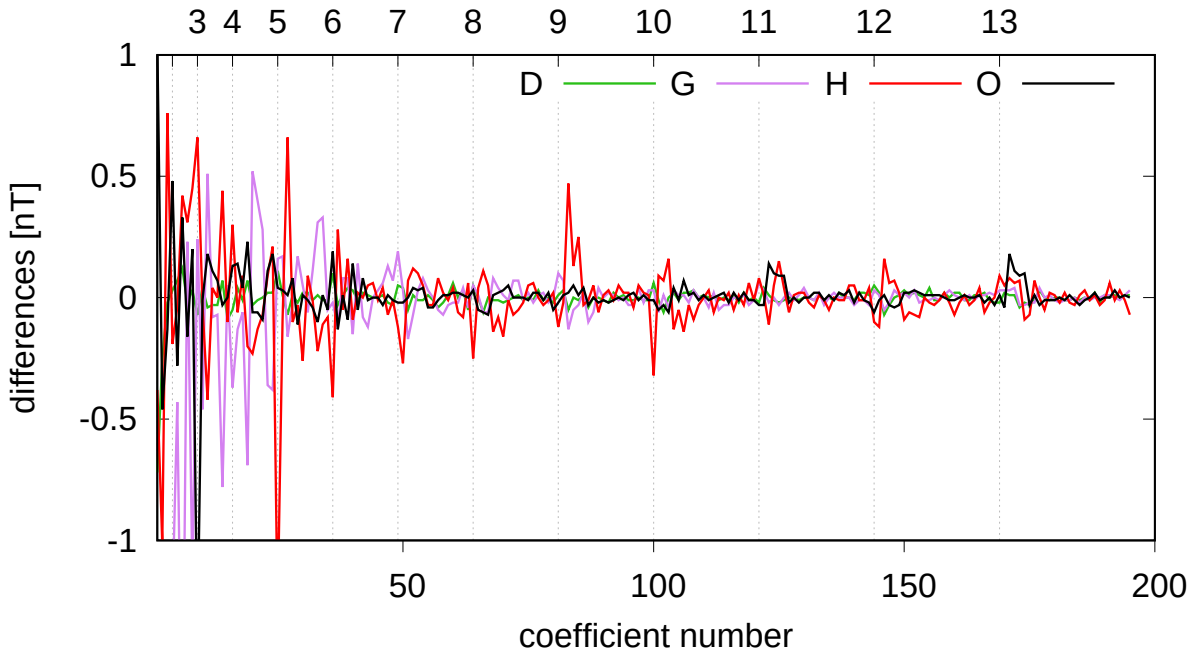

Figure 2: Differences of the Gauss coefficients of 4 candidate models; the candidate (D) with the smallest and the three models with the largest deviation from the mean model (see Table 1). The labels on the top axis refer to the spherical harmonic degree, and mark g_n^0 with $n = 1 \ldots 13$.

Model	A	B	C	D	E	F	G	
diff nT^2	4.38	-	3.38	1.99	3.98	2.70	56.35	
Model	H	I	J	K	L	M	N	O
diff nT^2	34.75	-	-	-	15.68	2.51	11.27	24.77

Table 1: Total intensities of the mean-candidates differences, DGRF 2015.

Model	[nT]	[nT]
A	-6.08	7.09
C	-5.70	6.53
D	-4.14	3.51
E	-6.72	5.29
F	-5.59	4.11
G	-15.79	16.45
H	-17.62	22.68
L	-13.60	6.98
M	-6.56	3.31
N	-9.96	9.14
O	-13.56	16.42

Table 2: Deviations from the mean DGRF candidate model of the radial component.

This is consistent with the specification of the DGRF/IGRF. The total field intensities of the difference fields range from 1.99 to 56.36 nT^2.

Figure 3 shows maps of the radial component of the difference fields. Corresponding values are given in Table 2.

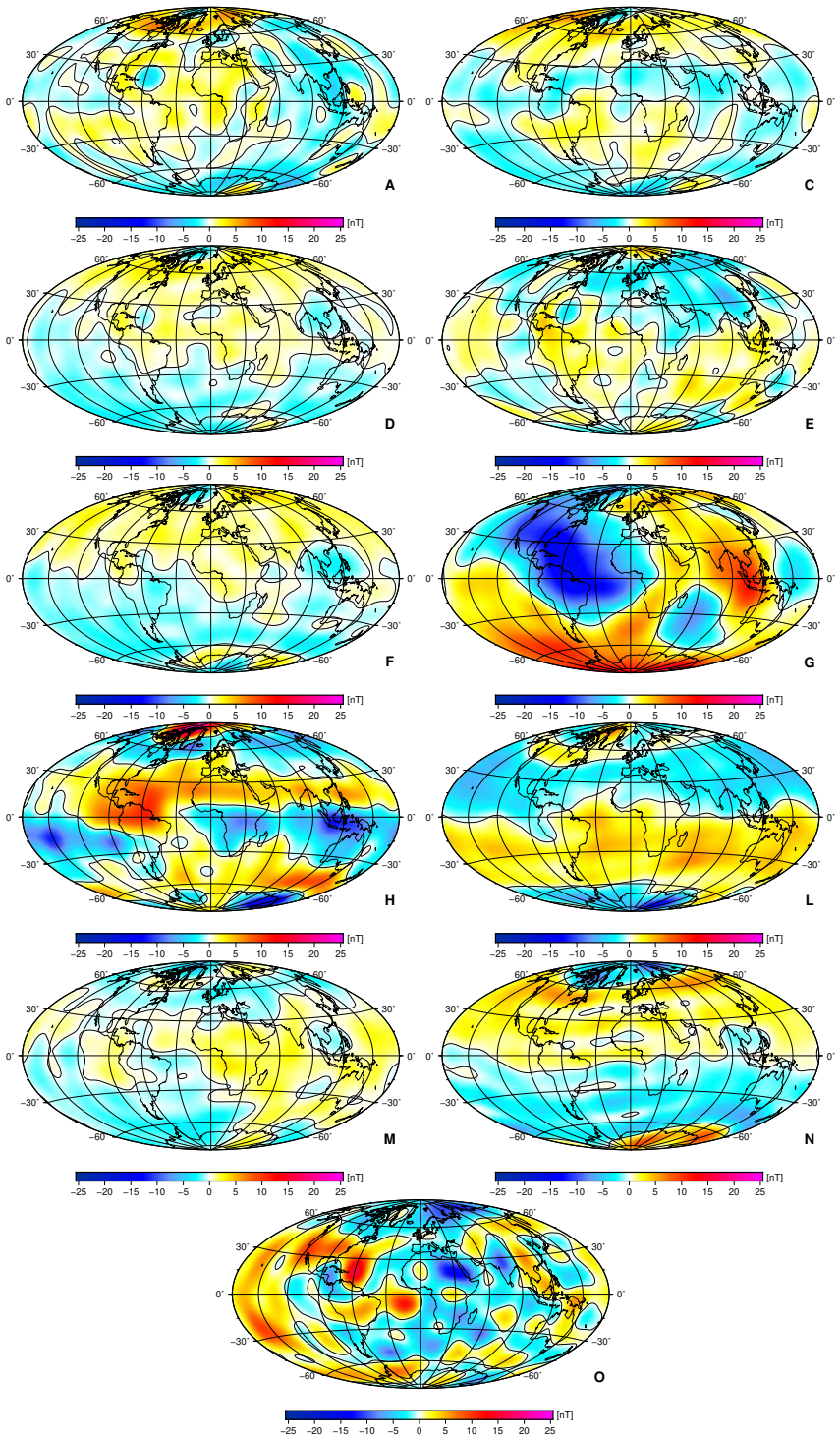

Figure 3: Radial component of the difference field at Earth's surface for the DGRF 2015 main field model candidates. Colors range from ± 25 nT.

3 IGRF 2020 candidate models

Figure 4 shows the radial component of the equally weighted average field of all IGRF candidates.

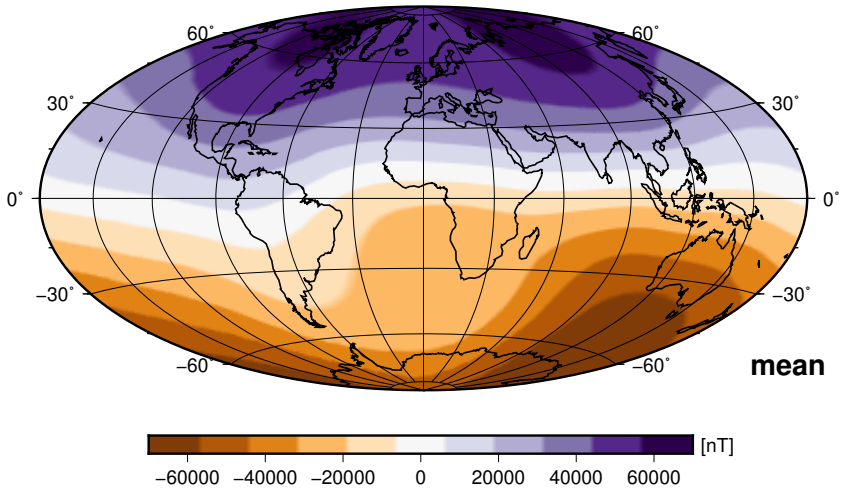

Figure 4: Radial component of the mean field at Earth's surface derived from all IGRF candidates.

This section provides results of the same analysis as in section 1. Figure 5 shows the Gauss coefficients of the difference fields in a range from -2 to 2 nT.

Model	A	B	C	D	E	F	G	
diff nT^2	20.38	109.00	29.24	12.81	219.57	23.39	78.27	
Model	H	I	J	K	L	M	N	O
diff nT^2	56.89	-	-	-	40.10	21.56	71.98	144.11

Table 3: Total intensities of the difference fields, IGRF 2020.

Figure 6 and Table 4 summarizes the analysis of the radial component of the difference fields.

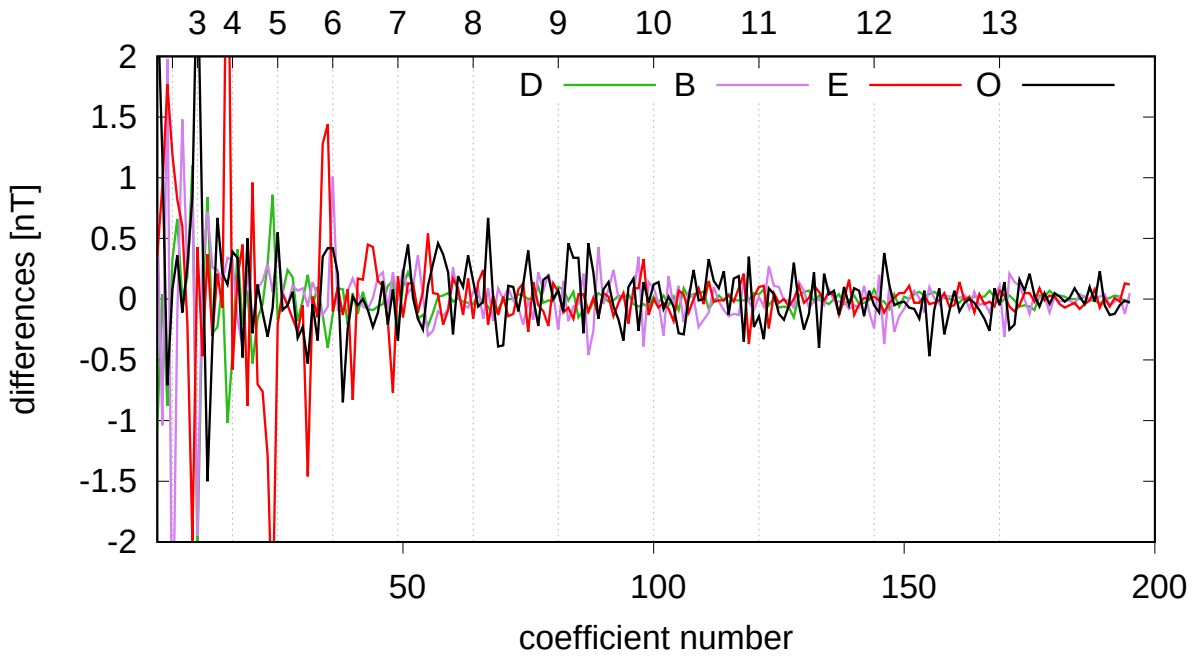

Figure 5: Differences of the Gauss coefficients of 4 candidate models; candidate (D) with the smallest and the three models with the largest deviation from the mean model (see Table 3).

Model	[nT]	[nT]
A	-9.29	11.16
B	-23.12	24.75
C	-19.57	21.18
D	-7.79	9.51
E	-50.59	46.38
F	-15.06	9.93
G	-20.93	16.49
H	-20.56	17.71
L	-10.72	12.58
M	-9.11	14.35
N	-70.34	16.87
O	-28.27	25.33

Table 4: Deviations from the mean IGRF candidate model of the radial component.

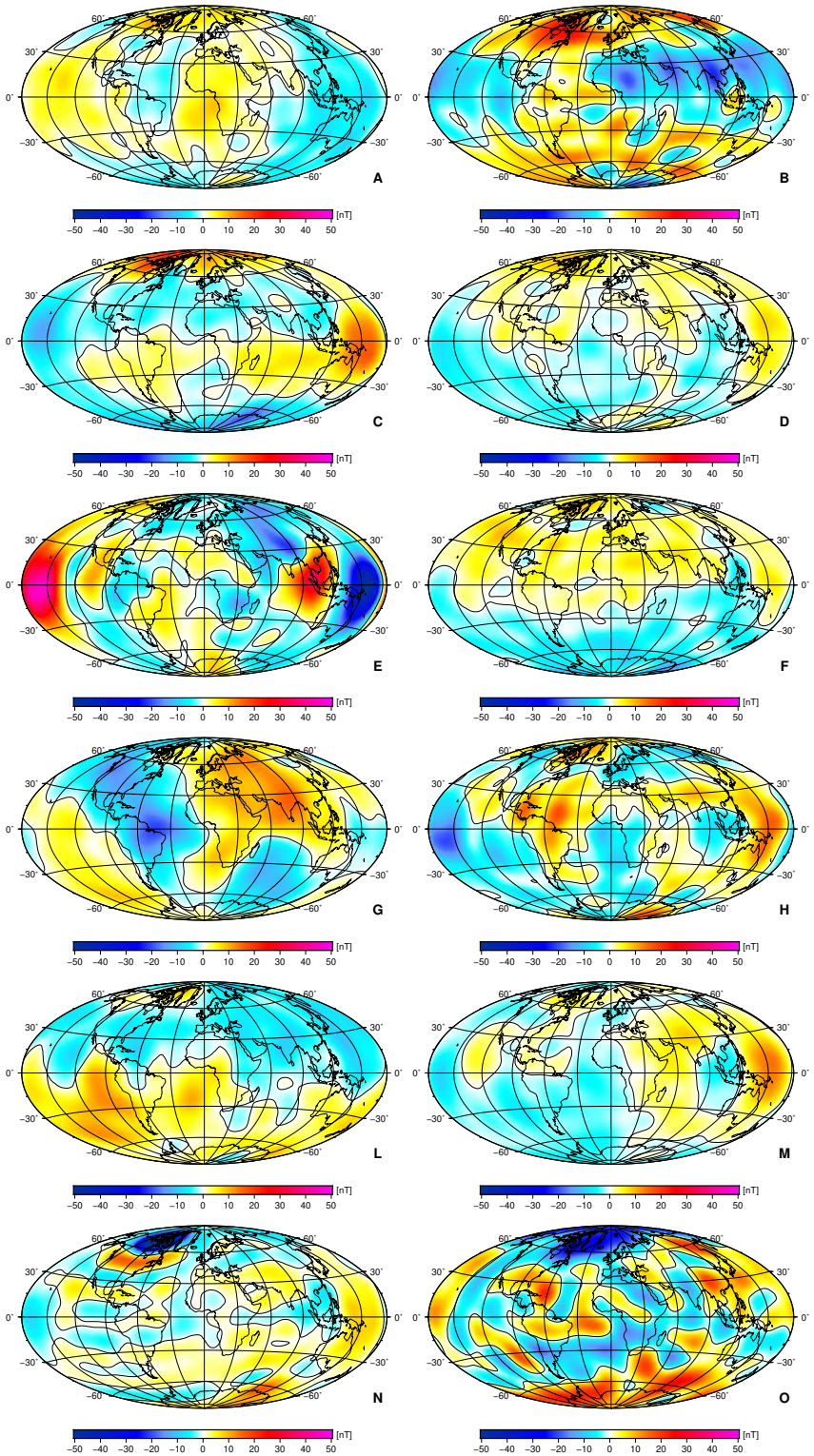

Figure 6: Radial component of the difference field at Earth's surface for the IGRF 2020 main field model candidates. Colors range from ± 50 nT.

Model	A	B	C	D	E	F	G	
diff $(\mathrm{nT/yr})^2$	68.90	-	151.19	16.11	89.37	54.82	63.03	
Model	H	I	J	K	L	M	N	O
diff $(\mathrm{nT/yr})^2$	269.22	351.93	45.24	44.00	713.15	46.25	44.03	439.63

Table 5: Total intensities of the mean-candidates differences, SV 2020-2025.

4 SV 2020 - 2025 candidate models

Figure 7 shows the radial component of the equally weighted averaged secular variation models.

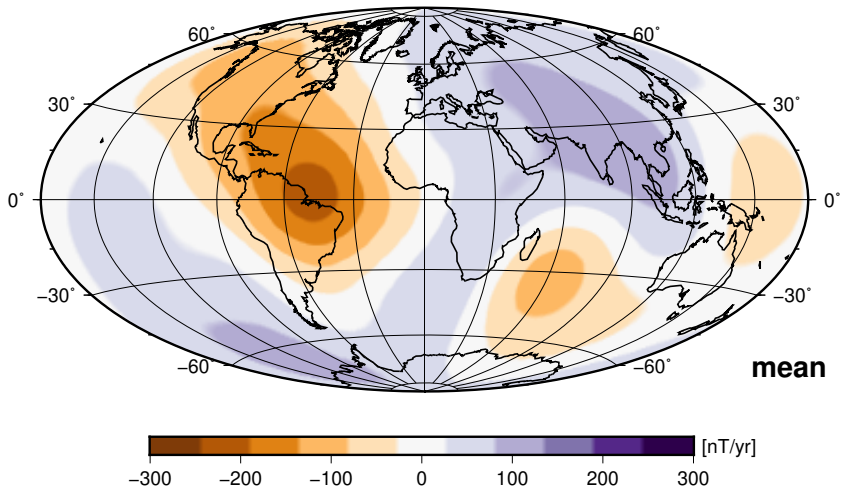

Figure 7: Radial component of the mean secular variation at Earth's surface derived from all secular variation candidates.

Figure 8 compares the deviation of Models I, N and O, with that of Model D. The largest deviations occur for the first three spherical harmonic degrees and their amplitudes are larger than ± 1nT.

The total intensity of the differences between a candidate model and the mean secular variation model ranges from 16.11 $(\mathrm{nT/yr})^2$ to 713.15 $(\mathrm{nT/yr})^2$. **Note, values given in Table 5 differ from those of Lowes, as I only consider the first 8 spherical harmonic degrees of the candidates models**. Some of these models provide spherical harmonic expansion up to spherical degree 13, which may have lead to different total intensity values.

Maps of the radial secular variation component of the difference fields are shown in Figure 9. The corresponding Table 6 lists extreme values of the maps for each candidate.

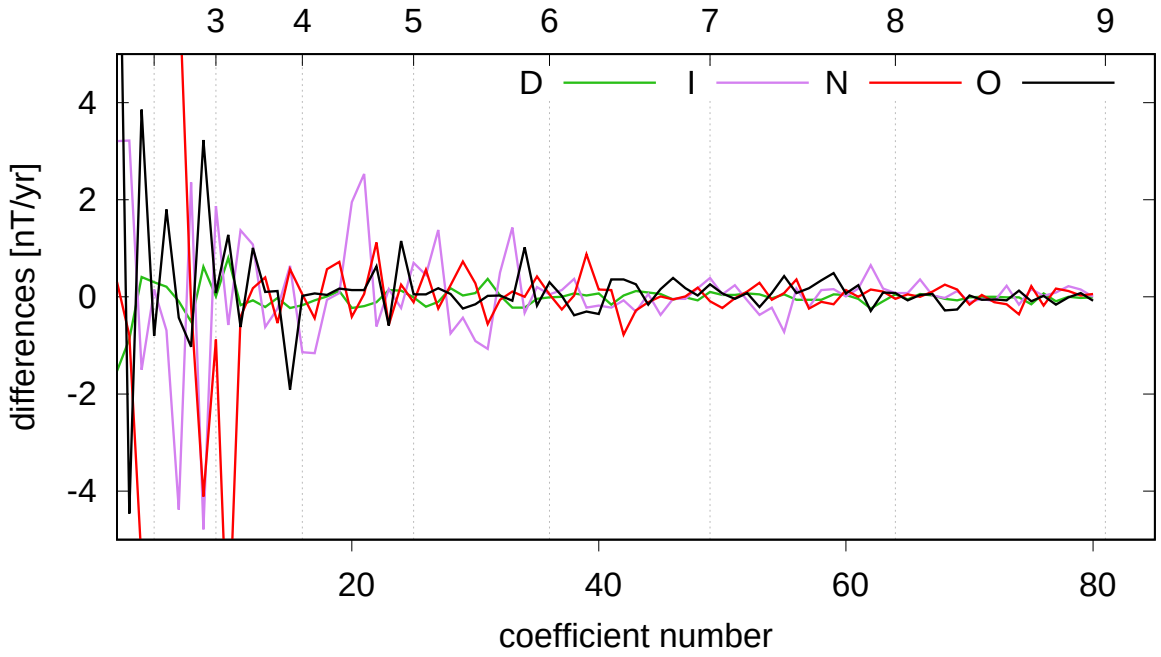

Figure 8: Differences of the Gauss coefficients of 4 candidate models, candidate (D) with the smallest and the three models with largest deviations from the mean model (see Table 5).

Model	[nT/yr]	[nT/yr]
A	-17.90	16.04
C	-31.34	33.64
D	-7.89	8.96
E	-29.55	29.59
F	-11.73	15.61
G	-11.75	19.78
H	-34.68	33.25
I	-29.94	40.18
J	-15.65	12.07
K	-10.18	17.43
L	-45.13	49.42
M	-14.27	23.82
N	-31.87	11.85
O	-30.47	30.62

Table 6: Deviation ranges of the candidate models from the mean secular variation model.

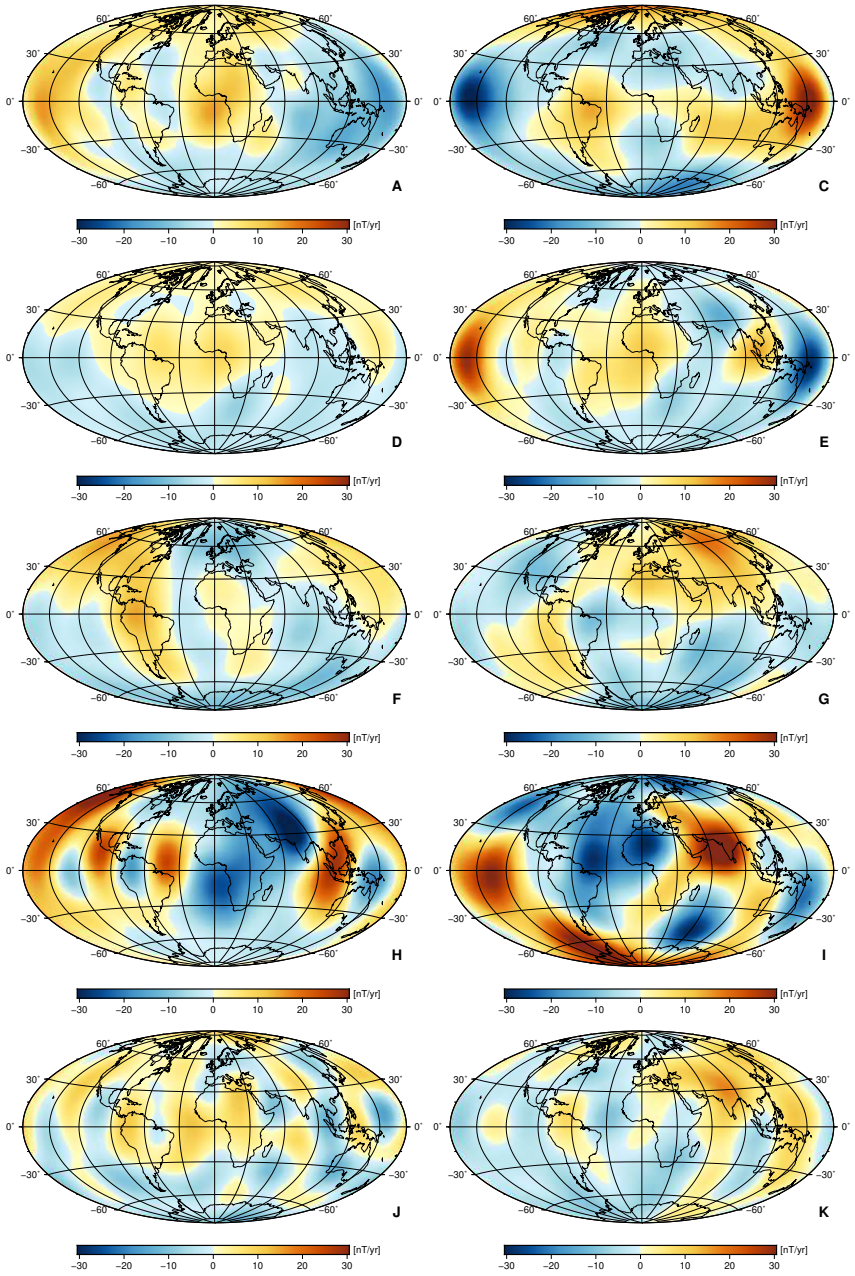

Figure 9: Radial secular variation component of the mean-candidates differences at Earth surface for the secular variation candidates. Colors range from ± 30 nT/yr.

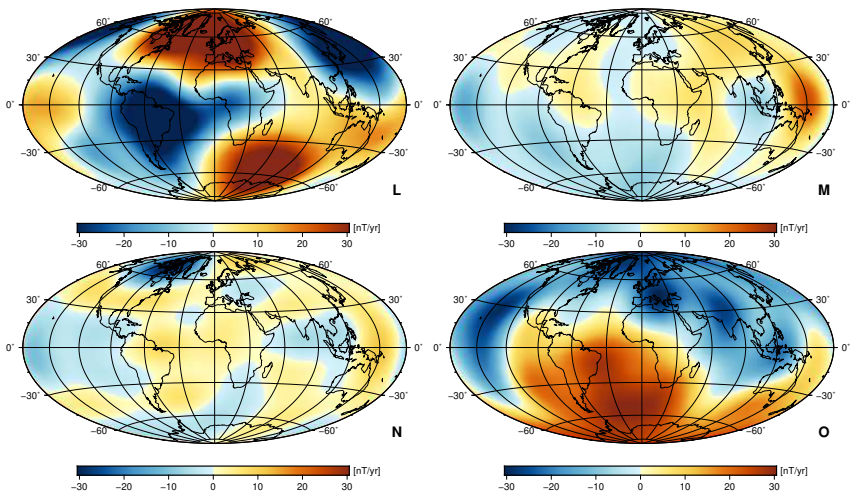

Figure 9 (Cont.)

5 Discussion and conclusions

5.1 DGRF and IGRF candidates

Model coefficients of the difference fields for DGRF and IGRF are mostly smaller than 1 nT for the large scale field, and on the range of ± 0.5 nT for the small scale field, see Figures 2, 5, the latter corresponds roughly to a measurement uncertainties of the same order. These uncertainties can be caused by different data selection schemes and the negligence of modeling other magnetic fields of ionospheric, magnetospheric and oceanic sources. These fields are known to generate magnetic field signatures of about ± 10 nT at Earth's surface.

Particularly, the effect by different data selection schemes may be present in the following models, DGRF: F, DGRF: L, DGRF: N, and (perhaps) DGRF: D. Their difference field shows a dipolar structure, with prominent differences in polar regions. That may hint seasonal variations caused by the selection of polar night time data, which are only available during polar winters. Models DGRF: L and DGRF: N show also imprints of the northern and southern auroral ovals.

The range of total field intensities of the mean-candidates differences is 1.99 to 56.36 nT^2. Where Model I shows the largest deviation from the mean main field model in 2015. However, all these values differ by 9 orders of magnitude to the total field intensity of the mean model, i.e. $21\times10^9 nT^2$.

The differences become larger for the IGRF 2020 candidate models; the total field intensity of the difference fields ranges from 12.81 to 219.57 nT^2. This is still at least 8 orders of magnitude to the total field intensity of the mean model.

The larger deviations of the IGRF candidate models could be simply due to the unavailability of geomagnetic field measurements after June 2019. Therefore, candidates represent an extrapolation of the solutions from the latest epoch to 2020.

Based on these comparisons, it is difficult to set a preference for one specific candidate models for DGRF and IGRF. Their differences to an equally weighted mean model could be regarded as insignificant as these represent only a very small fraction of the total field intensity.

5.2 Secular variation candidates

The evaluation of the secular variation candidates reveals larger disagreements between candidates and the arithmetic mean secular variation model. With a maximum difference of 713 $(nT/yr)^2$ (Model L). These disagreements are entirely due to different modeling strategies. Previous studies [1; 2; 3; 5] have indicated that the secular variation shows substantial variation on time scales shorter than 5 years. This may serve as a reason to exclude predictions of Models C, D, E, N and perhaps H that use linear extrapolation of the secular variation from 2019/2020 to the center epoch 2022.5. A linear extrapolation over 5 years (2019 - 2020) is not expected to recover this short term secular variation, especially not geomagnetic jerks. The remaining models apply forecasts that are based

on various data assimilation schemes (Models A, F, I, J, K, L, M), spline extrapolation (Model G) and singular spectrum analysis (Model O).

Table 7 provides the total intensities of differences between candidate models and the mean secular variation model. This mean secular variation model is derived as the equally weighted mean of 9 models that are not using a linear extrapolation of the secular variation from 2019/2020.

The radial component of the averaged secular variation from these 9 models are shown in Figure 10. The maxima of the radial component are the same as in Figure 7, i.e. -215.99 and 131.3 nT/yr.

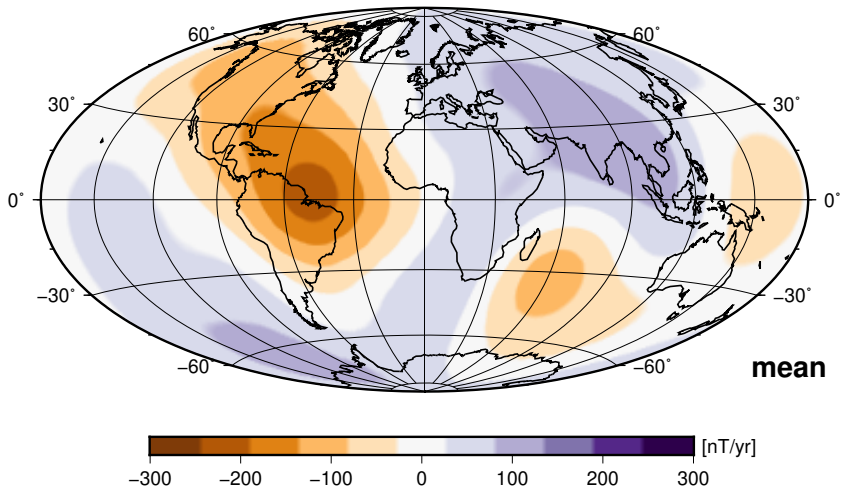

Figure 10: Radial component of the mean secular variation at Earth's surface derived from 9 secular variation candidates that are based on advanced forecasting methods.

Model	A	F	G	I	J	K	L	M	O
diff $(\mathrm{nT/yr})^2$	70.63	78.87	61.16	308.27	54.15	45.93	641.50	56.97	439.88

Table 7: Total intensities of the mean-candidates differences (SV 2020-2025) derived from models A, F, G, I, J, K, L, M and O.

The table shows that the candidates of Models I, L and O largely deviate from the mean secular variation model. Again, deviations from the mean model are due to different modeling philosophies, but the deviations of Models I, L, O account for almost 1% of the total intensity of the secular variation, which is 71820.35 $(\mathrm{nT/yr})^2$. The resulting radial component of the secular variation is shown in Figure 11. the range of this map is -221.49 to 130.09 nT/yr.

Based on this comparison, I would suggest to derive the final secular variation model for the period 2020 to 2025 by equally averaging Models A, F, G, J, K and M. These models represent the most developed stage of geomagnetic forecasting, and ensures an sophisticated description of the short-term secular variation.

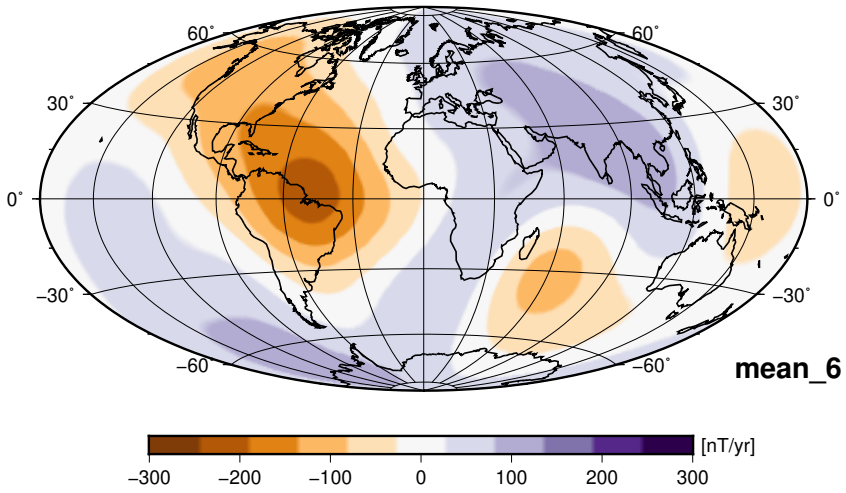

Figure 11: Radial component of the mean secular variation at Earth's surface derived from 6 secular variation candidates (A, F, G, J, K and M).

A Declination differences

The difference in Declination may be a particularly useful measure to quantify differences between mean and individual models, because the declination defined by the IGRF is used by scientific and non-scientific applications. Figure 12 shows the declination of the equally averaged DGRF candidate models.

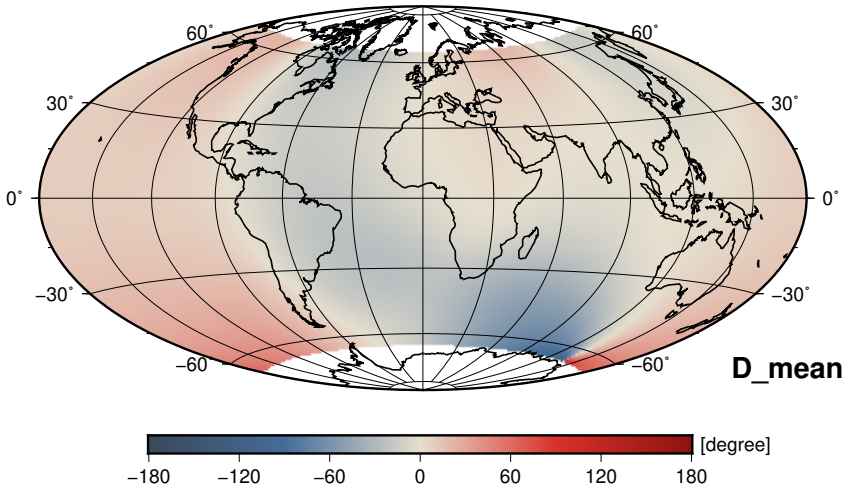

Figure 12: Declination of the mean model at Earth's surface, DGRF 2015.

The differences between the mean declination and the declination of the individual candidates are computed using a grid with 166845 grid points north of −65° Latitude, and south of −65° Latitude, excluding regions close to the magnetic poles. In polar regions the differences are largest and may account for several degrees. In other regions differences are below ± 6 arc minutes.

Figures 14 and 15 show the same analysis for the IGRF 2020 candidates. Here the differences are larger, but do not exceed 6 arc minutes in non-polar regions. However, the significance of these differences is not easy to evaluate, because a geomagnetic observer at an observatory can resolve 0.5 arc seconds (given ideal conditions). On other hand, navigational applications that use the geomagnetic declination rarely resolve 0.5 degree; even worse magneto-telluric field experiments or paleomagnetic drillings work with a precision of one to a few degrees in declination.

References

[1] Arnaud Chulliat, Patrick Alken, and Stefan Maus. Fast equatorial waves propagating at the top of the Earth's core. *Geophys. Res. Lett.*, 42(9):3321–3329, May 2015.

[2] V. Lesur, I. Wardinski, J. Baerenzung, and M. Holschneider. On the frequency spectra of the core magnetic field Gauss coefficients. *Phys. Earth Planet. Inter.*, 2:164–168, 2017.

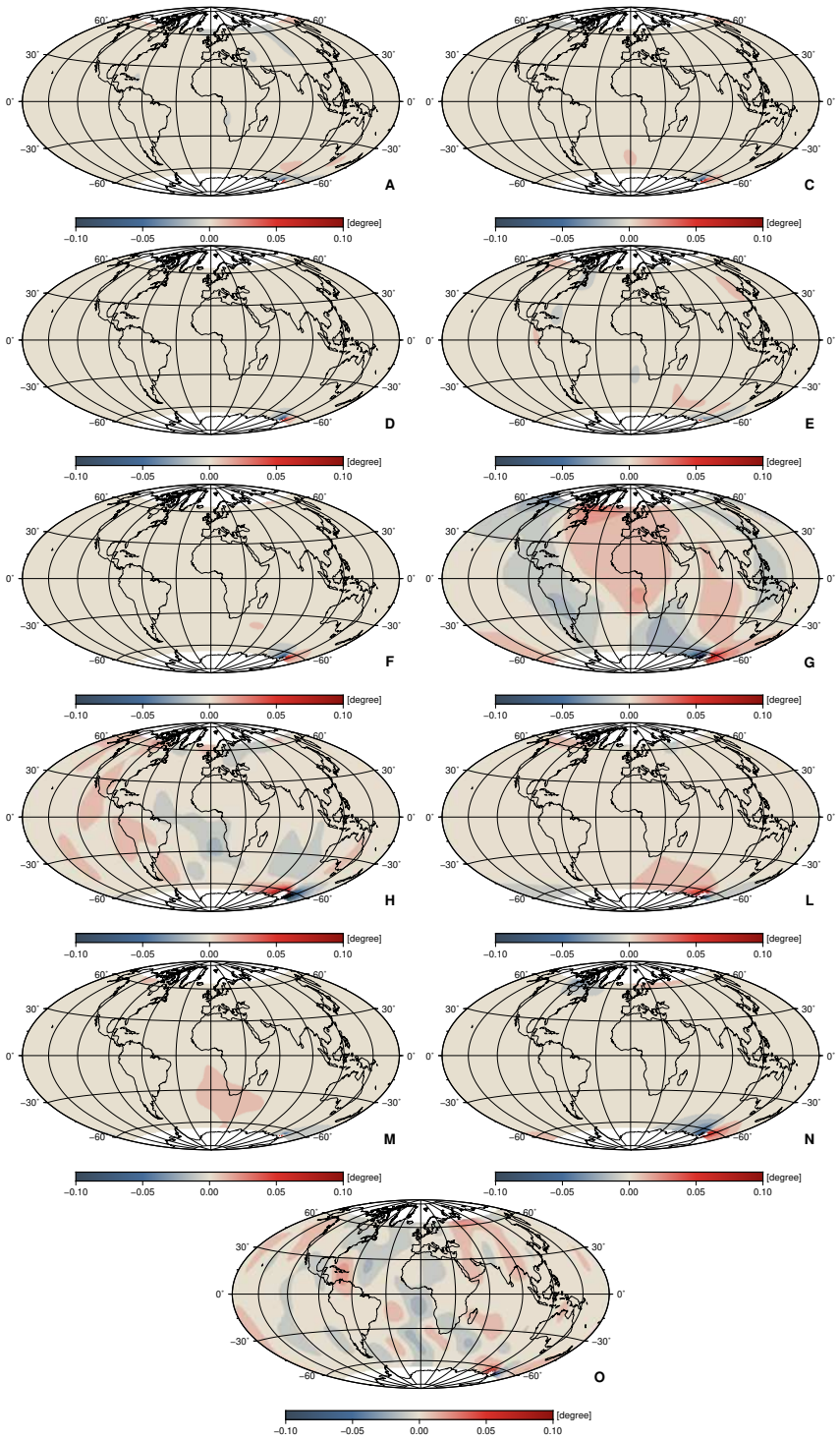

Figure 13: Differences in Declination between mean field model and candidates for the DGRF 2015. Colors range from ± 6 arc minutes.

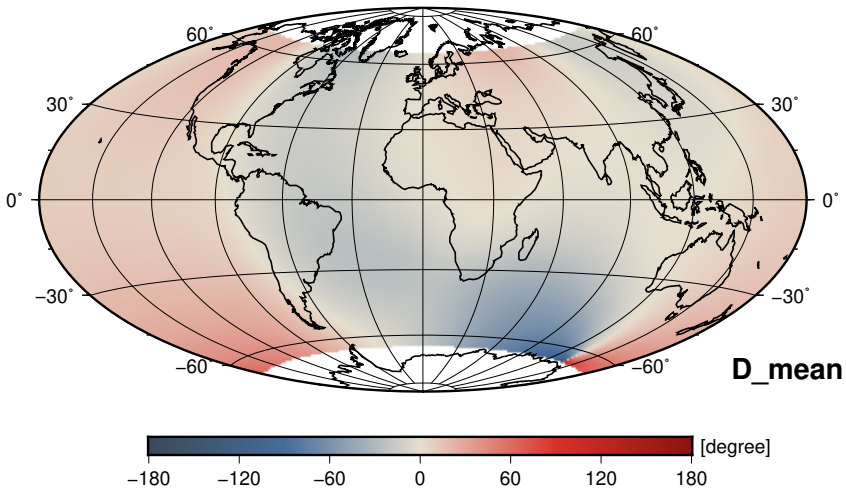

Figure 14: Declination of the mean model at Earth's surface, IGRF 2020.

[3] Anatoly Soloviev, Arnaud Chulliat, and Shamil Bogoutdinov. Detection of secular acceleration pulses from magnetic observatory data. *Phys. Earth Planet. Inter.*, 270:128–142, Sep 2017.

[4] Erwan Thébault, Christopher C. Finlay, Patrick Alken, Ciaran D. Beggan, Elisabeth Canet, Arnaud Chulliat, Benoit Langlais, Vincent Lesur, Frank J. Lowes, Chandrasekharan Manoj, Martin Rother, and Reyko Schachtschneider. Evaluation of candidate geomagnetic field models for IGRF-12. *Earth, Planets, and Space*, 67:112, Jul 2015.

[5] J. Miquel Torta, F. Javier Pavón-Carrasco, Santiago Marsal, and Christopher C. Finlay. Evidence for a new geomagnetic jerk in 2014. *Geophys. Res. Lett.*, 42(19):7933–7940, Oct 2015.

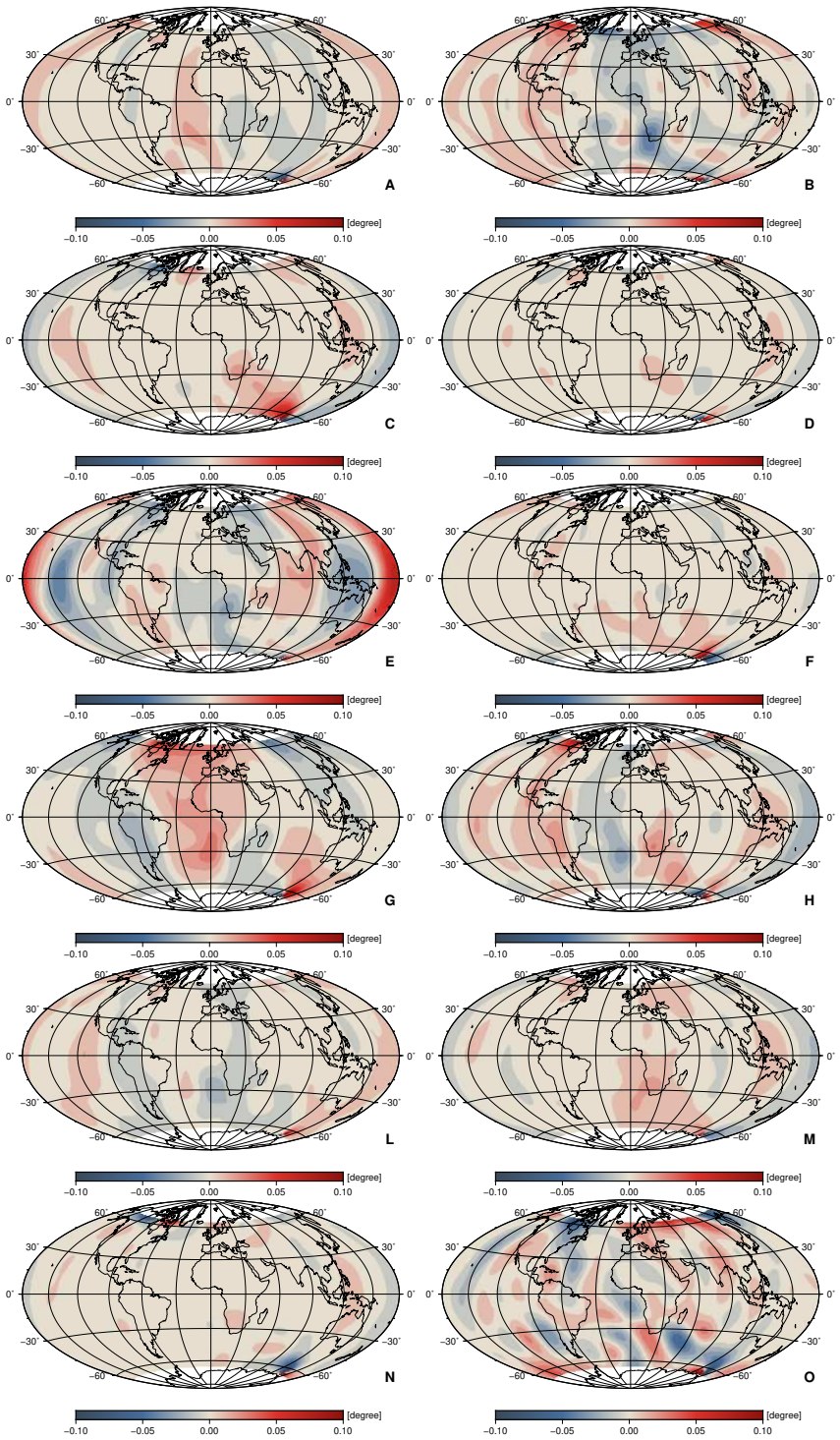

Figure 15: Differences in Declination between mean field model and candidates for the IGRF 2020. Colors range from ± 6 arc minutes.